

We are IntechOpen, the world's leading publisher of Open Access books Built by scientists, for scientists

6,900

Open access books available

186,000

International authors and editors

200M

Downloads

Our authors are among the

154

Countries delivered to

TOP 1%

most cited scientists

12.2%

Contributors from top 500 universities



WEB OF SCIENCE™

Selection of our books indexed in the Book Citation Index
in Web of Science™ Core Collection (BKCI)

Interested in publishing with us?
Contact book.department@intechopen.com

Numbers displayed above are based on latest data collected.
For more information visit www.intechopen.com



Super-Twisting Sliding Mode in Motion Control Systems

Jorge Rivera¹, Luis Garcia², Christian Mora³,
Juan J. Raygoza⁴ and Susana Ortega⁵

^{1,2,3,4}*Centro Universitario de Ciencias Exactas e Ingenierías, Universidad de Guadalajara*

⁵*Centro de Investigación y Estudios Avanzados del I.P.N. Unidad Guadalajara
México*

1. Introduction

Nowadays, the major advancements in the control of motion systems are due to the automatic control theory. Motion control systems are characterized by complex nonlinear dynamics and can be found in the robotic, automotive and electromechanical area, among others. In such systems it is always wanted to impose a desired behavior in order to cope with the control objectives that can go from velocity and position tracking to torque and current tracking among other variables. Motion control systems become vulnerable when the output tracking signals present small oscillations of finite frequency known as chattering. The chattering problem is harmful because it leads to low control accuracy; high wear of moving mechanical parts and high heat losses in power circuits. The chattering phenomenon can be caused by the deliberate use of classical sliding mode control technique. This control technique is characterized by a discontinuous control action with an ideal infinite frequency. When fast dynamics are neglected in the mathematical model such phenomenon can appear. Another situation responsible for chattering is due to implementation issues of the sliding mode control signal in digital devices operating with a finite sampling frequency, where the switching frequency of the control signal cannot be fully implemented. Despite of the disadvantage presented by the sliding mode control, this is a popular technique among control engineer practitioners due to the fact that introduces robustness to unknown bounded perturbations that belong to the control sub-space; moreover, the residual dynamic under the sliding regime, i.e., the sliding mode dynamic, can easily be stabilized with a proper choice of the sliding surface. A proof of their good performance in motion control systems can be found in the book by Utkin et al. (1999). A solution to this problem is the high order sliding mode (HOSM) technique, Levant (2005). This control technique maintains the same sliding mode properties (in this sense, first-order sliding mode) with the advantage of eliminating the chattering problem due to the continuous-time nature of the control action. The actual disadvantage of this control technique is that the stability proofs are based on geometrical methods since the Lyapunov function proposing results in a difficult task, Levant (1993). The work presented in Moreno & Osorio (2008) proposes quadratic like Lyapunov functions for a special case of second-order sliding mode controller, the super-twisting sliding mode controller (STSMC), making possible to obtain an explicit relation for the controller design parameters.

In this chapter, two motion control problems will be addressed. First, a position trajectory tracking controller for an under-actuated robotic system known as the Pendubot will be designed. Second, a rotor velocity and magnetic rotor flux modulus tracking controller will be designed for an induction motor.

The Pendubot (see Spong & Vidyasagar (1989)) is an under-actuated robotic system, characterized by having less actuators than links. In general, this can be a natural design due to physical limitations or an intentional one for reducing the robot cost. The control of such robots is more difficult than fully actuated ones. The Pendubot is a two link planar robot with a dc motor actuating in the first link, with the first one balancing the second link. The purpose of the Pendubot is research and education inside the control theory of nonlinear systems. Common control problems for the Pendubot are swing-up, stabilization and trajectory tracking. In this work, a super-twisting sliding mode controller for the Pendubot is designed for trajectory tracking, where the proper choice of the sliding function can easily stabilize the residual sliding mode dynamic. A novel Lyapunov function is used for a rigorous stability analysis of the controller here designed. Numeric simulations verify the good performance of the closed-loop system.

In the other hand, induction motors are widely used in industrial applications due to its simple mechanical construction, low service requirements and lower cost with respect to DC motors that are also widely used in the industrial field. Therefore, induction motors constitute a classical test bench in the automatic control theory framework due to the fact that represents a coupled MIMO nonlinear system, resulting in a challenging control problem. It is worth mentioning that there are several works that are based on a mathematical induction motor model that does not consider power core losses, implying that the induction motor presents a low efficiency performance. In order to achieve a high efficiency in power consumption one must take into consideration at least the power core losses in addition to copper losses; then, to design a control law under conditions obtained when minimizing the power core and copper losses. With respect to loss model based controllers, there is a main approach for modeling the core, as a parallel resistance. In this case, the resistance is fixed in parallel with the magnetization inductance, increasing the four electrical equations to six in the (α, β) stationary reference frame, Levi et al. (1995). In this work, one is compelled to design a robust controller-observer scheme, based on the super-twisting technique. A novel Lyapunov function is used for a rigorous stability analysis. In order to yield to a better performance of induction motors, the power core and copper losses are minimized. Simulations are presented in order to demonstrate the good performance of the proposed control strategy.

The remaining structure of this chapter is as follows. First, the sliding mode control will be revisited. Then, the Pendubot is introduced to develop the super-twisting controller design. In the following part, the induction motor model with core loss is presented, and the super-twisting controller is designed in an effort of minimizing the power losses. Finally some comments conclude this chapter.

2. Sliding mode control

The sliding mode control is a well documented control technique, and their fundamentals can be founded in the following references, Utkin (1993), Utkin et al. (1999), among others. Therefore in this section, the main features of this control technique are revisited in order to introduce the super-twisting algorithm.

The first order or classical sliding mode control is a two-step design procedure consisting of a sliding surface ($S = 0$) design with relative degree one w.r.t. the control (the control

appears explicitly in \dot{S}), and a discontinuous control action that ensures a sliding regime or a sliding mode. When the states of the system are confined in the sliding mode, i.e., the states of the system have reached the surface, the convergence happens in a finite-time fashion, moreover, the matched bounded perturbations are rejected. From this time instant the motion of the system is known as the sliding mode dynamic and it is insensitive to matched bounded perturbations. This dynamic is commonly characterized by a reduced set of equations. At the initial design stage, one must predict the sliding mode dynamic structure and then to design the sliding surface in order to stabilize it. It is worth mentioning that the sliding mode dynamic (commonly containing the output) is commonly asymptotically stabilized. This fact is sometimes confusing since one can expect to observe the finite-time convergence at the output of the system, but as mentioned above the finite-time convergence occurs at the designed surface. The main disadvantage of the classical sliding mode is the chattering phenomenon, that is characterized by small oscillations at the output of the system that can result harmful to motion control systems. The chattering can be developed due to neglected fast dynamics and to digital implementation issues.

In order to overcome the chattering phenomenon, the high-order sliding mode concept was introduced by Levant (1993). Let us consider a smooth dynamic system with an output function S of class C^{r-1} closed by a constant or dynamic discontinuous feedback as in Levant & Alelishvili (2007). Then, the calculated time derivatives $S, \dot{S}, \dots, S^{r-1}$, are continuous functions of the system state, where the set $S = \dot{S} = \dots = S^{r-1} = 0$ is non-empty and consists locally of Filippov trajectories. The motion on the set above mentioned is said to exist in r -sliding mode or r_{th} order sliding mode. The r_{th} derivative S^r is considered to be discontinuous or non-existent. Therefore the high-order sliding mode removes the relative-degree restriction and can practically eliminate the chattering problem.

There are several algorithms to realize HOSM. In particular, the 2_{nd} order sliding mode controllers are used to zero the outputs with relative degree two or to avoid chattering while zeroing outputs with relative degree one. Among 2_{nd} order algorithms one can find the sub-optimal controller, the terminal sliding mode controllers, the twisting controller and the super-twisting controller. In particular, the twisting algorithm forces the sliding variable S of relative degree two in to the 2-sliding set, requiring knowledge of \dot{S} . The super-twisting algorithm does not require \dot{S} , but the sliding variable has relative degree one. Therefore, the super-twisting algorithm is nowadays preferable over the classical sliding mode, since it eliminates the chattering phenomenon.

The actual disadvantage of HOSM is that the stability proofs are based on geometrical methods, since the Lyapunov function proposal results in a difficult task, Levant (1993). The work presented in Moreno & Osorio (2008) proposes quadratic like Lyapunov functions for the super-twisting controller, making possible to obtain an explicit relation for the controller design parameters. In the following lines this analysis will be revisited.

Let us consider the following SISO nonlinear scalar system

$$\dot{\sigma} = f(t, \sigma) + u \quad (1)$$

where $f(t, \sigma)$ is an unknown bounded perturbation term and globally bounded by $|f(t, \sigma)| \leq \delta |\sigma|^{1/2}$ for some constant $\delta > 0$. The super-twisting sliding mode controller for perturbation and chattering elimination is given by

$$\begin{aligned} u &= -k_1 \sqrt{|\sigma|} \text{sign}(\sigma) + v \\ \dot{v} &= -k_2 \text{sign}(\sigma). \end{aligned} \quad (2)$$

System (1) closed by control (2) results in

$$\begin{aligned}\dot{\sigma} &= -k_1\sqrt{|\sigma|}\text{sign}(\sigma) + v + f(t, \sigma) \\ \dot{v} &= -k_2\text{sign}(\sigma).\end{aligned}\quad (3)$$

Proposing the following candidate Lyapunov function:

$$\begin{aligned}\mathcal{V} &= 2k_2|\sigma| + \frac{1}{2}v^2 + \frac{1}{2}(k_1|\sigma|^{1/2}\text{sign}(\sigma) - v)^2 \\ &= \tilde{\zeta}^T P \tilde{\zeta}\end{aligned}$$

where $\tilde{\zeta}^T = (|\sigma|^{1/2}\text{sign}(\sigma) \ v)$ and

$$P = \frac{1}{2} \begin{pmatrix} 4k_2 + k_1^2 & -k_1 \\ -k_1 & 2 \end{pmatrix},$$

Its time derivative along the solution of (3) results as follows:

$$\dot{\mathcal{V}} = -\frac{1}{|\sigma|^{1/2}}\tilde{\zeta}^T Q \tilde{\zeta} + \frac{f(t, \sigma)}{|\sigma|^{1/2}}q_1^T \tilde{\zeta}$$

where

$$Q = \frac{k_1}{2} \begin{pmatrix} 2k_2 + k_1^2 & -k_1 \\ -k_1 & 1 \end{pmatrix},$$

$$q_1^T = (2k_2 + \frac{1}{2}k_1^2 \ -\frac{1}{2}k_1).$$

Applying the bounds for the perturbations as given in Moreno & Osorio (2008), the expression for the derivative of the Lyapunov function is reduced to

$$\dot{\mathcal{V}} = -\frac{k_1}{2|\sigma|^{1/2}}\tilde{\zeta}^T \tilde{Q} \tilde{\zeta}$$

where

$$\tilde{Q} = \begin{pmatrix} 2k_2 + k_1^2 - (\frac{4k_2}{k_1} + k_1)\delta & -k_1 + 2\delta \\ -k_1 + 2\delta & 1 \end{pmatrix}.$$

In this case, if the controller gains satisfy the following relations

$$k_1 > 2\delta, \quad k_2 > k_1 \frac{5\delta k_1 + 4\delta^2}{2(k_1 - 2\delta)},$$

then, $\tilde{Q} > 0$, implying that the derivative of the Lyapunov function is negative definite.

3. STSMC for an under-actuated robotic system

In this section a super-twisting sliding mode controller for the Pendubot is designed. The Pendubot is schematically shown in Figure 1.

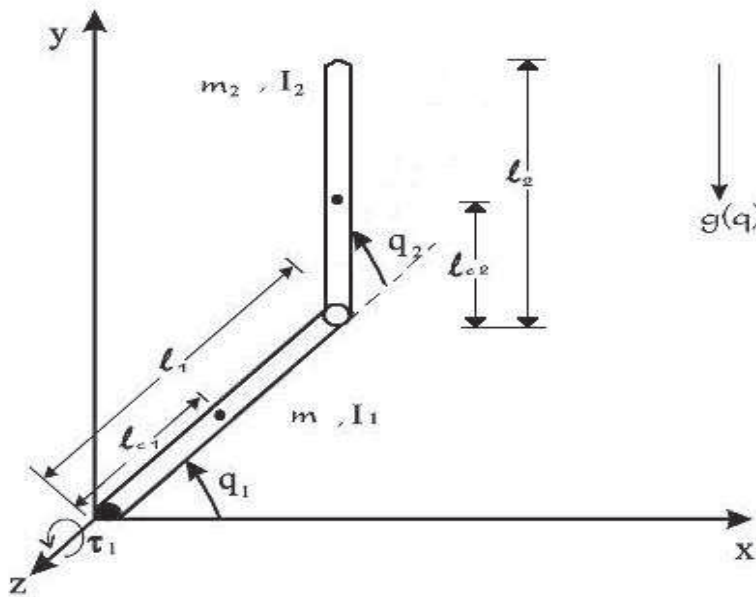


Fig. 1. Schematic diagram of the Pendubot.

3.1 Mathematical model of the Pendubot

The equation of motion for the Pendubot can be described by the following general Euler-Lagrange equation Spong & Vidyasagar (1989):

$$D(q)\ddot{q} + C(q, \dot{q}) + G(q) + F(\dot{q}) = \tau \tag{4}$$

where $q = [q_1, q_2]^T \in \mathbb{R}^n$ is the vector of joint variables (generalized coordinates), $q_1 \in \mathbb{R}^m$ represents the actuated joints, and $q_2 \in \mathbb{R}^{(n-m)}$ represents the unactuated ones. $D(q)$ is the $n \times n$ inertia matrix, $C(q, \dot{q})$ is the vector of Coriolis and centripetal torques, $G(q)$ contains the gravitational terms, $F(\dot{q})$ is the vector of viscous frictional terms, and τ is the vector of input torques. For the Pendubot system, the dynamic model (4) is particularized as

$$\begin{bmatrix} D_{11} & D_{12} \\ D_{12} & D_{22} \end{bmatrix} \begin{bmatrix} \ddot{q}_1 \\ \ddot{q}_2 \end{bmatrix} + \begin{bmatrix} C_1 \\ C_2 \end{bmatrix} + \begin{bmatrix} G_1 \\ G_2 \end{bmatrix} + \begin{bmatrix} F_1 \\ F_2 \end{bmatrix} = \begin{bmatrix} \tau_1 \\ 0 \end{bmatrix}$$

where $D_{11}(q_2) = m_1 l_{c1}^2 + m_2(l_1^2 + l_{c2}^2 + 2l_1 l_{c2} \cos q_2) + I_1 + I_2$, $D_{12}(q_2) = m_2(l_{c2}^2 + l_1 l_{c2} \cos q_2) + I_2$, $D_{22} = m_2 l_{c2}^2 + I_2$, $C_1(q_2, \dot{q}_1, \dot{q}_2) = -2m_2 l_1 l_{c2} \dot{q}_1 \dot{q}_2 \sin q_2 - m_2 l_1 l_{c2} \dot{q}_2^2 \sin q_2$, $C_2(q_2, \dot{q}_1) = m_2 l_1 l_{c2} \dot{q}_1^2 \sin q_2$, $G_1(q_1, q_2) = m_1 g l_{c1} \cos q_1 + m_2 g l_1 \cos q_1 + m_2 g l_{c2} \cos(q_1 + q_2)$, $G_2(q_1, q_2) = m_2 g l_{c2} \cos(q_1 + q_2)$, $F_1(\dot{q}_1) = \mu_1 \dot{q}_1$, $F_2(\dot{q}_2) = \mu_2 \dot{q}_2$, with m_1 and m_2 as the mass of the first and second link of the Pendubot respectively, l_1 is the length of the first link, l_{c1} and l_{c2} are the distance to the center of mass of link one and two respectively, g is the acceleration of gravity, I_1 and I_2 are the moment of inertia of the first and second link respectively about its centroids, and μ_1 and μ_2 are the viscous drag coefficients. The nominal values of the parameters are taken as follows: $m_1 = 0.8293$, $m_2 = 0.3402$, $l_1 = 0.2032$, $l_{c1} = 0.1551$, $l_{c2} = 0.1635125$, $g = 9.81$, $I_1 = 0.00595035$, $I_2 = 0.00043001254$, $\mu_1 = 0.00545$, $\mu_2 = 0.00047$. Choosing $x = (x_1 \ x_2 \ x_3 \ x_4)^T = (q_1 \ q_2 \ \dot{q}_1 \ \dot{q}_2)^T$ as the state vector, $u = \tau_1$ as the input, and x_2 as the output, the description of the system can be given in state space form

as:

$$\dot{x}(t) = f(x) + g(x)u(t) \quad (5)$$

$$e(x, w) = x_2 - w_2$$

$$\dot{w} = s(w) \quad (6)$$

where $e(x, w)$ is output tracking error, $w = (w_1, w_2)^T$, and w_2 as the reference signal generated by the known exosystem (6),

$$f(x) = \begin{pmatrix} f_1(x_3) \\ f_2(x_4) \\ f_3(x) \\ f_4(x_1, x_2, x_3) \end{pmatrix} = \begin{pmatrix} x_3 \\ x_4 \\ b_3(x_2)p_1(x) \\ b_4(x_2)p_2(x) \end{pmatrix},$$

$$g(x) = \begin{pmatrix} b_1 \\ b_2 \\ b_3(x_2) \\ b_4(x_2) \end{pmatrix} = \begin{pmatrix} 0 \\ 0 \\ \frac{D_{22}}{D_{11}(x_2)D_{22} - D_{12}^2(x_2)} \\ \frac{-D_{12}(x_2)}{D_{11}(x_2)D_{22} - D_{12}^2(x_2)} \end{pmatrix},$$

$$s(w) = \begin{pmatrix} \alpha w_2 \\ -\alpha w_1 \end{pmatrix},$$

$$p_1(x) = \frac{D_{12}(x_2)}{D_{22}} (C_2(x_2, x_3) + G_2(x_1, x_2) + F_2(x_4)) - C_1(x_2, x_3, x_4) - G_1(x_1, x_2) - F_1(x_3),$$

$$p_2(x) = \frac{D_{11}(x_2)}{D_{12}} (C_2(x_2, x_3) + G_2(x_1, x_2) + F_2(x_4)) - C_1(x_2, x_3, x_4) - G_1(x_1, x_2) - F_1(x_3).$$

3.2 Control design

Now, the steady-state zero output manifold $\pi(w) = (\pi_1(w), \pi_2(w), \pi_3(w), \pi_4(w))^T$ is introduced. Making use of its respective regulator equations:

$$\frac{\partial \pi_1(w)}{\partial w} s(w) = \pi_3(w) \quad (7)$$

$$\frac{\partial \pi_2(w)}{\partial w} s(w) = \pi_4(w) \quad (8)$$

$$\frac{\partial \pi_3(w)}{\partial w} s(w) = b_3(\pi_2(w))p_1(\pi(w)) + b_3(\pi_2(w))c(w) \quad (9)$$

$$\frac{\partial \pi_4(w)}{\partial w} s(w) = b_4(\pi_2(w))p_2(\pi(w)) + b_4(\pi_2(w))c(w) \quad (10)$$

$$0 = \pi_2(w) - w_2 \quad (11)$$

$$\pi/2 = \pi_1(w) + \pi_2(w) \quad (12)$$

with $c(w)$ as the steady-state value for $u(t)$ that will be defined in the following lines. From equation (11) one directly obtains $\pi_2(w) = w_2$, then, replacing $\pi_2(w)$ in equation (8) yields to $\pi_4(w) = -\alpha w_1$. For calculating $\pi_1(w)$ and $\pi_3(w)$, the solution of equations (7) and (9) are needed, but in general this is a difficult task, that it is commonly solved proposing an approximated solution as in Ramos et al. (1997) and Rivera et al. (2008). Thus, one proposes

the following approximated solution for $\pi_1(w)$

$$\begin{aligned} \pi_1(w) = & a_0 + a_1w_1 + a_2w_2 + a_3w_1^2 + a_4w_1w_2 + a_5w_2^2 + a_6w_1^3 \\ & + a_7w_1^2w_2 + a_8w_1w_2^2 + a_9w_2^3 + O^4(\|w\|_1) \end{aligned} \quad (13)$$

replacing (13) in (7) and choosing $\alpha = 0.3$ yields the approximated solution for $\pi_3(w)$

$$\begin{aligned} \pi_3(w) = & 0.3a_1w_2 - 0.3a_2w_1 + 0.6a_3w_1w_2 + 0.3a_4w_2^2 - 0.3a_4w_1^2 - 0.6a_5w_2w_1 + 0.9a_6w_1^2w_2 \\ & + 0.6a_7w_1w_2^2 - 0.3a_7w_1^3 + 0.3a_8w_2^3 - 0.6a_8w_1^2w_2 - 0.9a_9w_2^2w_1 + O^4(\|w\|_1). \end{aligned} \quad (14)$$

Calculating from (10) $c(w) = -p_2(\pi(w)) - \alpha^2w_2/b_4(\pi_2(w))$, and using it along with (14) in equation (9) and performing a series Taylor expansion of the right hand side of this equation around the equilibrium point $(\pi/2, 0, 0, 0)^T$, then, one can find the values a_i ($i = 0, \dots, 9$) if the coefficients of the same monomials appearing in both side of such equation are equalized. In this case, the coefficients results as follows: $a_0 = 1.570757$, $a_1 = -0.00025944$, $a_2 = -1.001871$, $a_3 = 0.0$, $a_4 = 0.0$, $a_5 = 0.0$, $a_6 = 0.0$, $a_7 = 0.001926$, $a_8 = 0.0$, $a_9 = -0.00001588$. It is worth mentioning that there is a natural steady-state constraint (12) for the Pendubot (see Figure 1), i.e., the sum of the two angles, q_1 and q_2 equals $\pi/2$. Using such constraint one can easily calculate $\pi_{1a}(w) = \pi/2 - \pi_2(w)$, and replacing $\pi_{1a}(w)$ in equation (7) yields to $\pi_{3a}(w) = \alpha w_1$, where the sub-index a refers to an alternative manifold. This result was simulated yielding to the same results when using the approximate manifold, which is to be expected if the motion of the pendubot is forced only along the geometric constraints.

Then, the variable $z = x - \pi(w) = (z^1, z^2)^T$ is introduced, where

$$\begin{aligned} z^1 = & (z_1, z_2, z_3)^T = (x_1 - \pi_1, x_2 - \pi_2, x_3 - \pi_3)^T \\ z^2 = & z_4 = x_4 - \pi_4. \end{aligned} \quad (15)$$

Then, system (5) is represented in the new variables (15) as

$$\begin{aligned} \dot{z}_1 = & z_3 + \pi_3 - \frac{\partial \pi_1}{\partial w} s(w) \\ \dot{z}_2 = & z_4 + \pi_4 - \frac{\partial \pi_2}{\partial w} s(w) \\ \dot{z}_3 = & b_3(z_2 + \pi_2)p_1(z + \pi) + b_3(z_2 + \pi_2)u - \frac{\partial \pi_3}{\partial w} s(w) \\ \dot{z}_4 = & b_4(z_2 + \pi_2)p_2(z + \pi) + b_4(z_2 + \pi_2)u - \frac{\partial \pi_4}{\partial w} s(w) \\ e(z, w) = & z_2 + \pi_2 - w_2 \\ \dot{w} = & s(w). \end{aligned} \quad (16)$$

We now define the sliding manifold:

$$\sigma = z_4 + \Sigma_1(z_1, z_2, z_3)^T, \Sigma_1 = (k_1, k_2, k_3) \quad (17)$$

and by taking its derivative along the solution of system (16) results in

$$\dot{\sigma} = \phi(w, z) + \gamma(w, z)u \quad (18)$$

where

$$\begin{aligned}\phi(w, z) &= b_4(z_2 + \pi_2)p_2(z + \pi) - \frac{\partial \pi_4}{\partial w}s(w) + k_1(z_3 + \pi_3 - \frac{\partial \pi_1}{\partial w}s(w)) \\ &\quad + k_2(z_4 + \pi_4 - \frac{\partial \pi_2}{\partial w}s(w)) + k_3(b_3(z_2 + \pi_2)p_1(z + \pi) - \frac{\partial \pi_3}{\partial w}s(w)), \\ \gamma(w, z) &= b_4(z_2) + \pi_2 + k_3b_3(z_2 + \pi_2),\end{aligned}$$

moreover, one can assume that $\phi(w, z)$ is an unknown perturbation term bounded by $|\phi(w, z)| \leq \delta_\phi$ with $\delta_\phi > 0$. At this point, one can propose the super-twisting controller as follows:

$$\begin{aligned}u &= (-\rho_1\sqrt{|\sigma|}\text{sign}(\sigma) + v)/\gamma(w, z) \\ \dot{v} &= -\rho_2\text{sign}(\sigma),\end{aligned}\tag{19}$$

and the system (18) closed-loop by control (19) results in

$$\begin{aligned}\dot{\sigma} &= -\rho_1\sqrt{|\sigma|}\text{sign}(\sigma) + v + \phi(w, z) \\ \dot{v} &= -\rho_2\text{sign}(\sigma),\end{aligned}\tag{20}$$

where the controller gains ρ_1 and ρ_2 are determined in a similar fashion to the procedure outlined in the previous section.

When the sliding mode occurs, i.e., $\sigma = 0$ one can easily determine from (17) that

$$z_4 = -k_1z_1 - k_2z_2 - k_3z_3$$

moreover the order of system (16) reduces in one, obtaining the sliding mode dynamic, i.e.,

$$\begin{aligned}\dot{z}^1 &= \phi_{sm}(w, z) = f_1(w, z) + g_1(w, z)u_{eq}|_{z_4=-k_1z_1-k_2z_2-k_3z_3} \\ e(z, w) &= z_2 + \pi_2 - w_2 \\ \dot{w} &= s(w).\end{aligned}\tag{21}$$

with

$$f_1 = \begin{pmatrix} z_3 + \pi_3 - \frac{\partial \pi_1}{\partial w}s(w) \\ z_4 + \pi_4 - \frac{\partial \pi_2}{\partial w}s(w) \\ b_3(z_2 + \pi_2)p_1(z + \pi) - \frac{\partial \pi_3}{\partial w}s(w) \end{pmatrix}, \quad g_1(w, z) = \begin{pmatrix} 0 \\ 0 \\ b_3(z_2 + \pi_2) \end{pmatrix},$$

and u_{eq} as the equivalent control calculated from $\dot{\sigma} = 0$ as

$$u_{eq} = -\frac{\phi(w, z)}{b_4(w, z) + k_3b_3(w, z)}.$$

The sliding function parameters k_1 , k_2 and k_3 should stabilize the sliding mode dynamic (21). For a proper choice of such constant parameters one can linearize the sliding mode dynamic

$$\dot{z}^1 = A_{sm}(\kappa)z^1$$

where $A_{sm}(\kappa) = \partial \phi_{sm} / \partial z^1 |_{z^1=0}$, with $\kappa = (k_1, k_2, k_3)$. In order to choose the design parameters, a polynomial with desired poles is proposed, $p_d(s) = (s - \lambda_1)(s - \lambda_2)(s - \lambda_3)$, such that, the coefficients of the characteristic equation that results from the matrix $A_{sm}(\kappa)$ are equalized with the ones related with $p_d(s)$, i. e., $\det(sI - A_{sm}(\kappa)) = p_d(s)$, in such manner one can find explicit relations for κ . In this case $\lim_{t \rightarrow \infty} z = 0$, accomplishing with the control objective.

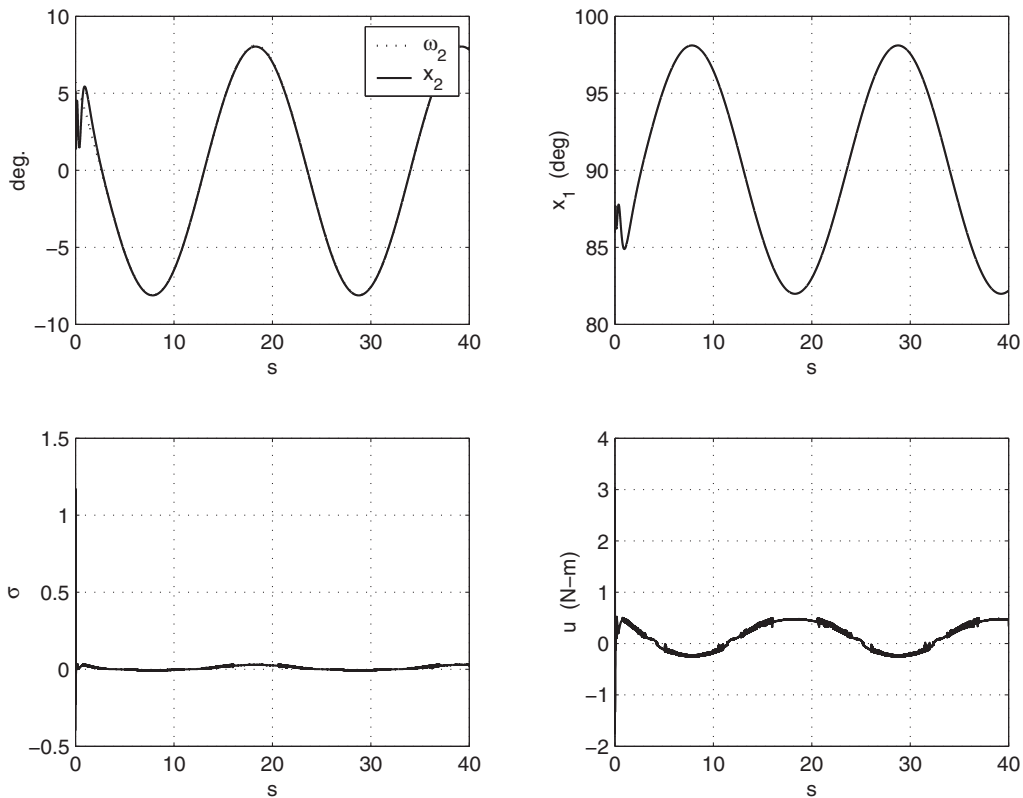


Fig. 2. a) Output tracking of the angle of the second link. b) Angle of the first link. c) Sliding surface. d) Control signal.

3.3 Simulations

In order to show the performance of the control methodology here proposed, simulations are carried out. The initial condition for the Pendubot is chosen as follows: $x_1(0) = 1.5$, $x_2(0) = 0.09$. Moreover, plant parameter variations are considered from time $t = 0$, due to possible measurement errors, therefore, the mass of the second link is considered as $m_2 = 0.5$, the moment of inertias of the first and second link are assumed to be $I_1 = 0.007$ and $I_2 = 0.0006$ respectively and the frictions of the first and second link are $\mu_1 = 0.01$ and $\mu_2 = 0.001$ respectively. The results are given in Fig. 2, where the robust performance of the super-twisting controller is put in evidence.

4. STSMC for induction motors with core loss

4.1 Induction motor model with core loss

In this section a super-twisting sliding mode controller for the induction motor is designed for copper and core loss minimization. Now we show the nonlinear affine representation for the induction motor with core loss in the stationary (α, β) reference frame taken from Rivera Dominguez et al. (2010):

$$\begin{aligned} \frac{d\omega}{dt} &= \eta_0(\psi_\alpha i_\beta - \psi_\beta i_\alpha) - \frac{Tl}{J} \\ \frac{d\psi_\alpha}{dt} &= -\eta_4 \psi_\alpha - Np\omega \psi_\beta + \eta_4 L_m i_{\alpha, Lm} \end{aligned}$$

$$\begin{aligned}
\frac{d\psi_\beta}{dt} &= -\eta_4\psi_\beta + Np\omega\psi_\alpha + \eta_4L_m i_{\beta,Lm} \\
\frac{di_{\alpha,Lm}}{dt} &= -(\eta_1 + \eta_2)i_{\alpha,Lm} + \frac{\eta_1}{L_m}\psi_\alpha + \eta_2i_\alpha \\
\frac{di_{\beta,Lm}}{dt} &= -(\eta_1 + \eta_2)i_{\beta,Lm} + \frac{\eta_1}{L_m}\psi_\beta + \eta_2i_\beta \\
\frac{di_\alpha}{dt} &= -(R_s\eta_3 + \eta_5)i_\alpha - \eta_1\eta_3\psi_\alpha \\
&\quad + (\eta_5 + \eta_1\eta_3L_m)i_{\alpha,Lm} + \eta_3v_\alpha \\
\frac{di_\beta}{dt} &= -(R_s\eta_3 + \eta_5)i_\beta - \eta_1\eta_3\psi_\beta \\
&\quad + (\eta_5 + \eta_1\eta_3L_m)i_{\beta,Lm} + \eta_3v_\beta
\end{aligned} \tag{22}$$

where

$$\begin{aligned}
\eta_0 &= \frac{3L_m Np}{2J(L_r - L_m)}, \quad \eta_1 = \frac{R_c}{L_r - L_m}, \\
\eta_2 &= \frac{R_c}{L_m}, \quad \eta_3 = \frac{1}{L_s - L_m}, \\
\eta_4 &= \frac{R_r}{L_r - L_m}, \quad \eta_5 = \frac{R_c}{L_s - L_m}.
\end{aligned}$$

with ω as the rotor velocity, v_α, v_β are the stator voltages, i_α, i_β are the stator currents, $i_{\alpha,Lm}, i_{\beta,Lm}$ are the magnetization currents and ψ_α, ψ_β are the rotor fluxes, with N_p as the number of pole pairs, R_s, R_r and R_c as the stator, rotor and core resistances respectively, L_l, L_l_r and L_m as the stator leakage, rotor leakage and magnetizing inductances respectively.

4.2 Transformation to the (d, q) rotating frame

Now, the induction motor model (22) will be transformed to the well known (d, q) reference frame by means of the following change of coordinates

$$\begin{aligned}
\begin{bmatrix} i_d \\ i_q \end{bmatrix} &= e^{-J\theta_\psi} \begin{bmatrix} i_\alpha \\ i_\beta \end{bmatrix}, \quad \begin{bmatrix} \psi_d \\ \psi_q \end{bmatrix} = e^{-J\theta_\psi} \begin{bmatrix} \psi_\alpha \\ \psi_\beta \end{bmatrix} \\
\begin{bmatrix} i_{dL_m} \\ i_{qL_m} \end{bmatrix} &= e^{-J\theta_\psi} \begin{bmatrix} i_{\alpha L_m} \\ i_{\beta L_m} \end{bmatrix}, \quad \begin{bmatrix} v_\alpha \\ v_\beta \end{bmatrix} = e^{J\theta_\psi} \begin{bmatrix} v_d \\ v_q \end{bmatrix}
\end{aligned}$$

where

$$e^{-J\theta_\psi} = \begin{bmatrix} \cos \theta_\psi & \sin \theta_\psi \\ -\sin \theta_\psi & \cos \theta_\psi \end{bmatrix}$$

with

$$\theta_\psi = \arctan \left(\frac{\psi_\beta}{\psi_\alpha} \right).$$

The field oriented or (d, q) model of the induction motor with core loss is now shown

$$\begin{aligned}
 \dot{\theta}_\psi &= n_p \omega + \frac{\eta_4 L_m i_{qL_m}}{\psi_d} \\
 \frac{d\omega}{dt} &= \eta_0 i_q \psi_d - \frac{Tl}{J} \\
 \frac{d\psi_d}{dt} &= -\eta_4 \psi_d + \eta_4 L_m i_{dL_m} \\
 \frac{di_{dL_m}}{dt} &= -(\eta_1 + \eta_2) i_{dL_m} + \frac{\eta_1 \psi_d}{L_m} + \eta_2 i_d + i_{qL_m} \dot{\theta} \\
 \frac{di_{qL_m}}{dt} &= -(\eta_1 + \eta_2) i_{qL_m} + \eta_2 i_q + i_{dL_m} \dot{\theta} \\
 \frac{di_d}{dt} &= -(R_s \eta_3 + \eta_5) i_d - \eta_1 \eta_3 \psi_d + (\eta_5 + \eta_1 \eta_3 L_m) i_{dL_m} + \eta_3 v_d + i_q \dot{\theta} \\
 \frac{di_q}{dt} &= -(R_s \eta_3 + \eta_5) i_q + (\eta_5 + \eta_1 \eta_3 L_m) i_{qL_m} + \eta_3 v_q - i_d \dot{\theta}
 \end{aligned} \tag{23}$$

The *control problem* is to force the rotor angular velocity ω and the square of the rotor flux modulus $\psi_m = \psi_\alpha^2 + \psi_\beta^2$ to track some desired references ω_r and $\psi_{m,r}$, ensuring at the same time load torque rejection. The control problem will be solved in a subsequent subsection by means of a super-twisting sliding mode controller.

4.2.1 Optimal rotor flux calculation

The copper and core losses are obtained by the corresponding resistances and currents. Therefore, the power lost in copper and core are expressed as follows:

$$P_L = \frac{3}{2} R_s (i_{d,s}^2 + i_{q,s}^2) + \frac{3}{2} R_r (i_{d,r}^2 + i_{q,r}^2) + \frac{3}{2} R_c (i_{d,Rc}^2 + i_{q,Rc}^2)$$

where $i_{d,r}$ and $i_{q,r}$ are the currents flowing through the rotor, $i_{d,Rc}$ and $i_{q,Rc}$ are the currents flowing through the resistance that represents the core. Since P_L is a positive-definite function can be considered as a cost function and then to be minimized with any desired variables, in this case the most suitable is the rotor flux, i. e.,

$$\frac{\partial P_L}{\partial \psi_d} = 0.$$

The resulting rotor flux component is given of the following form

$$\psi_{d,o} = \left(\frac{R_r L_m}{R_r + R_c} + \frac{R_c L_r}{R_r + R_c} \right) i_{dL_m} - \frac{R_c (L_r - L_m) i_d}{R_r + R_c}$$

4.3 Control design

In order to solve the posed control problem using the super-twisting sliding mode approach, we first derive the expression of the tracking error dynamics $z_1 = \omega - \omega_r$, $z_2 = \psi_m - \psi_{d,o}$ which are the output which we want to force to zero. The error tracking dynamic for the rotor velocity results as

$$z_1 = \eta_0 \psi_d i_q - \frac{Tl}{J} - \dot{\omega}_r. \tag{24}$$

Proposing a desired dynamic for z_1 of the following form

$$\dot{z}_1 = \eta_0 \psi_d i_q - \frac{Tl}{J} - \dot{\omega}_r = k_1 z_1$$

one can calculate i_q as a reference signal, i. e., i_{qr}

$$i_{qr} = \frac{\left(k_1 z_1 + \frac{Tl}{J} + \dot{\omega}_r\right)}{\eta_0 \psi_d} \quad (25)$$

in order to force the current component i_q to track its reference current, one defines the following tracking error

$$\xi_2 = i_q - i_{qr} \quad (26)$$

and taking the derivative of this error

$$\dot{\xi}_2 = \phi_q + \eta_3 v_q \quad (27)$$

where

$$\phi_q = -(R_s \eta_3 + \eta_5) i_q + (\eta_5 + \eta_1 \eta_3 L_m) i_{qL_m} - i_d \dot{\theta}_\psi - i_{qr} \dot{r}$$

is considered to be a bounded unknown perturbation term, i.e., $|\phi_q| \leq \delta_q$ with $\delta_q > 0$. The control law is proposed of the following form:

$$\begin{aligned} v_q &= (-\rho_{q,1} \sqrt{|\xi_2|} \text{sign}(\xi_2) + v_q) / \eta_3 \\ \dot{v}_q &= -\rho_{q,2} \text{sign}(\xi_2), \end{aligned} \quad (28)$$

and the system (27) closed-loop by control (28) results in

$$\begin{aligned} \dot{\xi}_2 &= -\rho_{q,1} \sqrt{|\xi_2|} \text{sign}(\xi_2) + v_q + \phi_q \\ \dot{v}_q &= -\rho_{q,2} \text{sign}(\xi_2), \end{aligned} \quad (29)$$

where the controller gains $\rho_{q,1}$ and $\rho_{q,2}$ are determined in a similar fashion to procedure outlined in the previous section. Now, from (26) one can write i_q as follows

$$i_q = \xi_2 + i_{qr}$$

and when substituting it along with (25) in (24) yields to

$$\dot{z}_1 = k_1 z_1 + \eta_0 \psi_d \xi_2.$$

Finally, collecting the equations

$$\begin{aligned} \dot{z}_1 &= k_1 z_1 + \eta_0 \psi_d \xi_2 \\ \dot{\xi}_2 &= -\rho_{q,1} \sqrt{|\xi_2|} \text{sign}(\xi_2) + v_q + \phi_q \\ \dot{v}_q &= -\rho_{q,2} \text{sign}(\xi_2). \end{aligned}$$

When the sliding mode occurs, i.e., $\xi_2 = 0$, the sliding mode dynamic results as:

$$\dot{z}_1 = k_1 z_1$$

and that with a proper choice of k_1 , one can lead to $z_1 = 0$.

Let us consider the second output z_2 , where its dynamic results as follows:

$$\dot{z}_2 = -\eta_4\psi_d + \eta_4L_m\dot{i}_{dL_m} - \dot{\psi}_{dr}, \quad (30)$$

note that the relative degree for z_2 is three, therefore in order to cope with the relative degree of z_1 , one proposes the following desired dynamic for z_2

$$\dot{z}_2 = -\eta_4\psi_d + \eta_4L_m\dot{i}_{dL_m} - \dot{\psi}_{dr} = k_2z_2 + z_3$$

where the new variable z_3 is calculated as:

$$z_3 = -\eta_4\psi_d + \eta_4L_m\dot{i}_{dL_m} - \dot{\psi}_{dr} - k_2z_2.$$

Taking the derivative of z_3 and assigning a desired dynamic

$$\begin{aligned} \dot{z}_3 = & \dot{i}_dL_m \left(-\eta_4^2L_m - \eta_4\eta_1L_m - \eta_4\eta_2L_m - k_2\eta_4L_m \right) + \dot{\psi}_d \left(\eta_4^2 + \eta_4\eta_1 + k_2\eta_4 \right) \\ & + \eta_4\eta_2L_m\dot{i}_d + \eta_4L_m\dot{i}_{qL_m}\dot{\theta}_\psi - \ddot{\psi}_{dr} + k_2\dot{\psi}_{dr} = k_3z_3 \end{aligned} \quad (31)$$

then, one can calculate i_d as a reference current, i. e., i_{dr}

$$\begin{aligned} i_{dr} = & \frac{k_3z_3 - \dot{i}_dL_m \left(-\eta_4^2L_m - \eta_4\eta_1L_m - \eta_4\eta_2L_m - k_2\eta_4L_m \right) - \dot{\psi}_d \left(\eta_4^2 + \eta_4\eta_1 + k_2\eta_4 \right)}{\eta_4\eta_2L_m} \\ & + \frac{-\eta_4L_m\dot{i}_{qL_m}\dot{\theta}_\psi + \ddot{\psi}_{dr} - k_2\dot{\psi}_{dr}}{\eta_4\eta_2L_m}. \end{aligned} \quad (32)$$

Defining the tracking error for the current d component

$$\xi_1 = i_d - i_{dr} \quad (33)$$

and by taking its derivative, i. e.,

$$\dot{\xi}_1 = \phi_d + \eta_3v_d \quad (34)$$

where

$$\phi_d = - (R_s\eta_3 + \eta_5) i_d - \eta_1\eta_3\psi_d + (\eta_5 + \eta_1\eta_3L_m) i_{dL_m} + i_q\dot{\theta}_\psi - \dot{i}_{dr}$$

is considered to be a bounded unknown perturbation term, i.e., $|\phi_d| \leq \delta_d$ with $\delta_d > 0$. The control law is proposed of the following form:

$$\begin{aligned} v_d = & (-\rho_{d,1}\sqrt{|\xi_1|}\text{sign}(\xi_1) + v_d) / \eta_3 \\ \dot{v}_d = & -\rho_{d,2}\text{sign}(\xi_1), \end{aligned} \quad (35)$$

and the system (34) closed-loop by control (35) results in

$$\begin{aligned} \dot{\xi}_1 = & -\rho_{d,1}\sqrt{|\xi_1|}\text{sign}(\xi_1) + v_d + \phi_d \\ \dot{v}_d = & -\rho_{d,2}\text{sign}(\xi_1), \end{aligned} \quad (36)$$

where the controller gains $\rho_{d,1}$ and $\rho_{d,2}$ are determined in a similar fashion to procedure outlined in the previous section. Now, from (33) one can write

$$i_d = \xi_1 + i_{dr}$$

and replacing it in (31) along with (32) yields to

$$\dot{z}_3 = k_3 z_3 + \eta_4 \eta_2 L_m \zeta_1.$$

Finally, collecting the equations

$$\begin{aligned} \dot{z}_2 &= k_2 z_2 + z_3 \\ \dot{z}_3 &= k_3 z_3 + \eta_4 \eta_2 L_m \zeta_1 \\ \dot{\zeta}_1 &= -\rho_{d,1} \sqrt{|\zeta_1|} \text{sign}(\zeta_1) + v_d + \phi_d \\ \dot{v}_d &= -\rho_{d,2} \text{sign}(\zeta_1). \end{aligned}$$

When the sliding mode occurs, i.e., $\zeta_1 = 0$, the closed-loop channel reduces its order:

$$\begin{aligned} \dot{z}_2 &= k_2 z_2 + z_3 \\ \dot{z}_3 &= k_3 z_3 \end{aligned}$$

one can see that the determination of k_2, k_3 , is easily achieved in order to lead to $z_2 = 0$.

4.4 Observer design

The first problem with the control strategy here developed is that the measurements of the rotor fluxes and magnetization currents are not possible. This problem is solved using an sliding mode observer. The second problem concerns the estimation of the load torque, where a classical Luemberger observer is designed.

The proposed sliding mode observer for rotor fluxes and magnetization currents is proposed based on (22) as follows:

$$\begin{aligned} \frac{d\hat{\psi}_\alpha}{dt} &= -\eta_4 \hat{\psi}_\alpha - N p \omega \hat{\psi}_\beta + \eta_4 L_m \hat{i}_{\alpha,Lm} + \rho_\alpha v_\alpha \\ \frac{d\hat{\psi}_\beta}{dt} &= -\eta_4 \hat{\psi}_\beta + N p \omega \hat{\psi}_\alpha + \eta_4 L_m \hat{i}_{\beta,Lm} + \rho_\beta v_\beta \\ \frac{d\hat{i}_{\alpha,Lm}}{dt} &= -(\eta_1 + \eta_2) \hat{i}_{\alpha,Lm} + \frac{\eta_1}{L_m} \hat{\psi}_\alpha + \eta_2 i_\alpha + \lambda_\alpha v_\alpha \\ \frac{d\hat{i}_{\beta,Lm}}{dt} &= -(\eta_1 + \eta_2) \hat{i}_{\beta,Lm} + \frac{\eta_1}{L_m} \hat{\psi}_\beta + \eta_2 i_\beta + \lambda_\beta v_\beta \\ \frac{d\hat{i}_\alpha}{dt} &= -(R_s \eta_3 + \eta_5) \hat{i}_\alpha - \eta_1 \eta_3 \hat{\psi}_\alpha \\ &\quad + (\eta_5 + \eta_1 \eta_3 L_m) \hat{i}_{\alpha,Lm} + \eta_3 v_\alpha + v_\alpha \\ \frac{d\hat{i}_\beta}{dt} &= -(R_s \eta_3 + \eta_5) \hat{i}_\beta - \eta_1 \eta_3 \hat{\psi}_\beta \\ &\quad + (\eta_5 + \eta_1 \eta_3 L_m) \hat{i}_{\beta,Lm} + \eta_3 v_\beta + v_\beta \end{aligned}$$

where $\rho_\alpha, \rho_\beta, \lambda_\alpha$ and λ_β are the observer design parameters, and v_α and v_β are the injected inputs to the observer that will be defined in the following lines. Now one defines the

estimation errors, $\tilde{\psi}_\alpha = \psi_\alpha - \hat{\psi}_\alpha$, $\tilde{\psi}_\beta = \psi_\beta - \hat{\psi}_\beta$, $\tilde{i}_{\alpha,Lm} = i_{\alpha,Lm} - \hat{i}_{\alpha,Lm}$, $\tilde{i}_{\beta,Lm} = i_{\beta,Lm} - \hat{i}_{\beta,Lm}$, $\tilde{i}_\alpha = i_\alpha - \hat{i}_\alpha$ and $\tilde{i}_\beta = i_\beta - \hat{i}_\beta$, whose dynamics can be expressed as:

$$\begin{aligned} \frac{d\tilde{\psi}_\alpha}{dt} &= -\eta_4\tilde{\psi}_\alpha - Np\omega\tilde{\psi}_\beta + \eta_4L_m\tilde{i}_{\alpha,Lm} - \rho_\alpha v_\alpha \\ \frac{d\tilde{\psi}_\beta}{dt} &= -\eta_4\tilde{\psi}_\beta + Np\omega\tilde{\psi}_\alpha + \eta_4L_m\tilde{i}_{\beta,Lm} - \rho_\beta v_\beta \\ \frac{d\tilde{i}_{\alpha,Lm}}{dt} &= -(\eta_1 + \eta_2)\tilde{i}_{\alpha,Lm} + \frac{\eta_1}{L_m}\tilde{\psi}_\alpha - \lambda_\alpha v_\alpha \\ \frac{d\tilde{i}_{\beta,Lm}}{dt} &= -(\eta_1 + \eta_2)\tilde{i}_{\beta,Lm} + \frac{\eta_1}{L_m}\tilde{\psi}_\beta - \lambda_\beta v_\beta \\ \frac{d\tilde{i}_\alpha}{dt} &= -(R_s\eta_3 + \eta_5)\tilde{i}_\alpha - \eta_1\eta_3\tilde{\psi}_\alpha \\ &\quad + (\eta_5 + \eta_1\eta_3L_m)\tilde{i}_{\alpha,Lm} - v_\alpha \\ \frac{d\tilde{i}_\beta}{dt} &= -(R_s\eta_3 + \eta_5)\tilde{i}_\beta - \eta_1\eta_3\tilde{\psi}_\beta \\ &\quad + (\eta_5 + \eta_1\eta_3L_m)\tilde{i}_{\beta,Lm} - v_\beta. \end{aligned} \quad (37)$$

Since the stator currents are measurable variables, one can choose the observer injection as $v_\alpha = l_\alpha \text{sign}(\tilde{i}_\alpha)$ and $v_\beta = l_\beta \text{sign}(\tilde{i}_\beta)$. From the derivative of the following Lyapunov candidate function $\mathcal{V}_o = \frac{1}{2}(\tilde{i}_\alpha^2 + \tilde{i}_\beta^2)$ along the trajectories of (37), one can easily determine the following bounds, $l_\alpha > |\eta_1\eta_3\tilde{\psi}_\alpha - (\eta_5 + \eta_1\eta_3L_m)\tilde{i}_{\alpha,Lm}|$ and $l_\beta > |\eta_1\eta_3\tilde{\psi}_\beta - (\eta_5 + \eta_1\eta_3L_m)\tilde{i}_{\beta,Lm}|$ that guarantees the convergence of \tilde{i}_α and \tilde{i}_β towards zero in finite time. When the sliding mode occurs, i. e., $\dot{\tilde{i}}_\alpha = \dot{\tilde{i}}_\beta = 0$ one can calculate the equivalent control for the injected signals from $\dot{\tilde{i}}_\alpha = 0$ and $\dot{\tilde{i}}_\beta = 0$ as $v_{\alpha,eq} = -\eta_1\eta_3\tilde{\psi}_\alpha + (\eta_5 + \eta_1\eta_3L_m)\tilde{i}_{\alpha,Lm}$, $v_{\beta,eq} = -\eta_1\eta_3\tilde{\psi}_\beta + (\eta_5 + \eta_1\eta_3L_m)\tilde{i}_{\beta,Lm}$, then, the sliding mode dynamic can be obtained by replacing the calculated equivalent controls, resulting in a linear time-variant dynamic system, $\dot{\epsilon} = A_o(\omega)\epsilon$, where $\epsilon = (\tilde{\psi}_\alpha \ \tilde{\psi}_\beta \ \tilde{i}_{\alpha,Lm} \ \tilde{i}_{\beta,Lm})^T$,

$$A_o = \begin{pmatrix} A_{o,11} & A_{o,12} \\ A_{o,21} & A_{o,22} \end{pmatrix}$$

with

$$\begin{aligned} A_{o,11} &= \begin{pmatrix} \rho_\alpha\eta_1\eta_3 - \eta_4 & -Np\omega \\ Np\omega & \rho_\beta\eta_1\eta_3 - \eta_4 \end{pmatrix}, \\ A_{o,12} &= \begin{pmatrix} \eta_4L_m - \rho_\alpha\gamma & 0 \\ 0 & \eta_4L_m - \rho_\beta\gamma \end{pmatrix}, \\ A_{o,21} &= \begin{pmatrix} \frac{\eta_1}{L_m} + \lambda_\alpha\eta_1\eta_3 & 0 \\ 0 & \frac{\eta_1}{L_m} + \lambda_\beta\eta_1\eta_3 \end{pmatrix}, \\ A_{o,22} &= \begin{pmatrix} -\eta_1 - \eta_2 - \lambda_\alpha\gamma & 0 \\ 0 & -\eta_1 - \eta_2 - \lambda_\beta\gamma \end{pmatrix}, \\ \gamma &= \eta_5 + \eta_1\eta_3L_m. \end{aligned}$$

In order to choose the design parameters, a polynomial with desired poles is proposed, $p_d(s) = (s - p_1)(s - p_2)(s - p_3)(s - p_4)$, such that, the coefficients of the characteristic equation that results from the matrix A_o are equalized with the ones related with $p_d(s)$, i. e., $\det(sI - A_o) = p_d(s)$, moreover, one can assume that the rotor velocity is constant, therefore the design parameters are easily determined. This will guarantee that $\lim_{t \rightarrow \infty} \epsilon(t) = 0$.

For the load torque estimation we consider that it is slowly varying, so one can assume it is constant, i. e., $\dot{T}l = 0$. This fact can be valid since the electric dynamic of the motor is faster than the mechanical one. Therefore, one proposes the following observer based on rotor velocity and stator current measurements

$$\begin{aligned} \frac{d\hat{\omega}}{dt} &= \eta_0(\hat{\psi}_\alpha i_\beta - \hat{\psi}_\beta i_\alpha) - \frac{\hat{T}l}{J} + l_1(\omega - \hat{\omega}) \\ \frac{d\hat{T}l}{dt} &= l_2(\omega - \hat{\omega}). \end{aligned}$$

Defining the estimation errors as $e_\omega = \omega - \hat{\omega}$ and $e_{Tl} = Tl - \hat{T}l$ one can determine the estimation error dynamic

$$\begin{pmatrix} \dot{e}_\omega \\ \dot{e}_{Tl} \end{pmatrix} = \begin{pmatrix} -l_1 & -\frac{1}{J} \\ -l_2 & 0 \end{pmatrix} \begin{pmatrix} e_\omega \\ e_{Tl} \end{pmatrix} + \eta_0 \begin{pmatrix} \tilde{\psi}_\alpha i_\beta - \tilde{\psi}_\beta i_\alpha \\ 0 \end{pmatrix}. \quad (38)$$

When the estimation errors for the rotor fluxes in (37) are zero, equation (38) reduces to

$$\begin{pmatrix} \dot{e}_\omega \\ \dot{e}_{Tl} \end{pmatrix} = \begin{pmatrix} -l_1 & -\frac{1}{J} \\ -l_2 & 0 \end{pmatrix} \begin{pmatrix} e_\omega \\ e_{Tl} \end{pmatrix} \quad (39)$$

where l_1 and l_2 can easily be determined in order to yield to $\lim_{t \rightarrow \infty} e_\omega(t) = 0$ and $\lim_{t \rightarrow \infty} e_{Tl}(t) = 0$.

4.5 Simulations

In this section we verify the performance of the proposed control scheme by means of numeric simulations.

We consider an induction motor with the following nominal parameters: $R_r = 10.1 \Omega$, $R_s = 14 \Omega$, $R_c = 1 \text{ k}\Omega$, $L_s = 400 \times 10^{-3} \text{ H}$, $L_r = 412.8 \times 10^{-3} \text{ H}$, $L_m = 377 \times 10^{-3} \text{ H}$, $J = 0.01 \text{ Kg m}^2$.

Hence, $\eta_1 = 27,932.96 \Omega/\text{H}$, $\eta_2 = 2,652.51 \Omega/\text{H}$, $\eta_3 = 43.47 \text{ H}^{-1}$, $\eta_4 = 282.12 \Omega/\text{H}$ and $\eta_5 = 43,478.26 \Omega/\text{H}$.

A load torque Tl of 5 Nm, with decrements of 1 Nm and 2 Nm at 8 s and 12 s respectively, has been considered in simulations. The reference velocity signal increases from 0 to 188.5 rad/s in the first 5 s and then remains constant, while the rotor flux modulus reference signal is directly taken from the calculated optimal flux.

A good tracking performance by the proposed controller can be appreciated in Figures 3 and 4. In Fig. 5 the power lost in copper and core is shown in the case of using the optimal flux modulus and the predicted open-loop steady state values in the cases of considering or not the core, this is a common practice when dealing with the control of the rotor flux in induction motors. From this figure one can observe a low power lost in copper and core when using the optimal flux, also one can note in Fig. 4 that the less is the load torque the lower is the flux level and as a consequence the power lost is reduced.

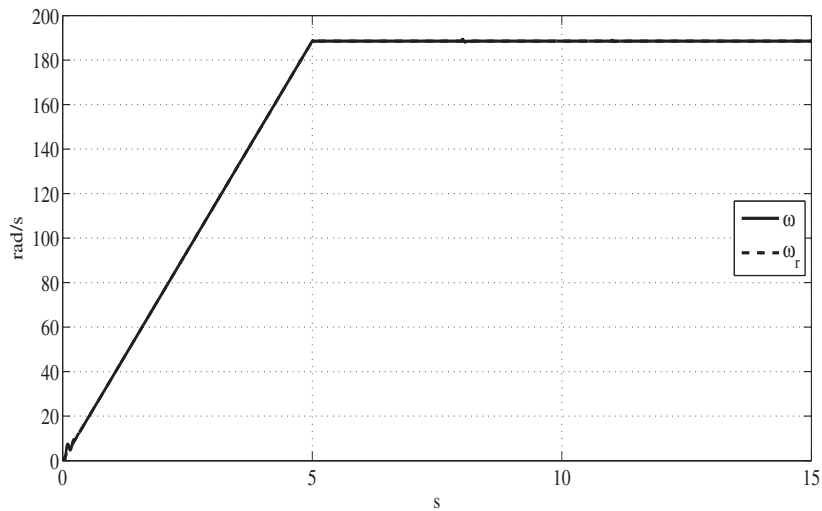


Fig. 3. Closed-loop velocity tracking of the proposed controller.

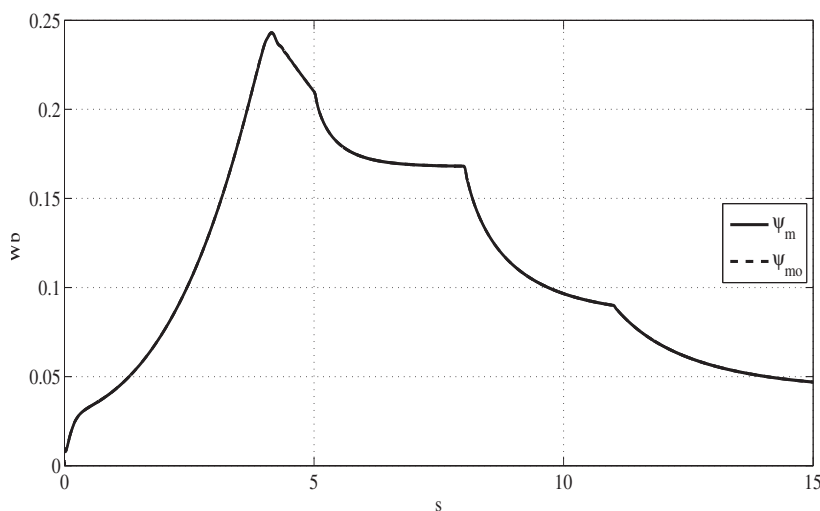


Fig. 4. Closed-loop optimal flux tracking of the proposed controller.

5. Conclusions

In this chapter the super-twisting algorithm and its application to motion control systems is shown. An under-actuated robotic system known as the Pendubot was closed-loop with a super-twisting controller. The procedure can easily be generalized to such type of motion systems. For that, one must consider the following generic steps: find the steady state for all states, then, based on the dynamic of the steady state errors one proposes an sliding function that linearly stabilizes the sliding mode dynamic. For the induction motor motion control, the (d, q) reference frame allows to decouple the control problem simplifying the control design. In each channel, a cascade strategy of defining first the output tracking error and then a desired current that shapes the dynamic of such output. Therefore, the sliding surface is simply chosen as a deviation of the current and its desired current. This strategy can be applied to all type of electric motors. In both scenarios, the super-twisting algorithm facilitates the motion control design and eliminates the chattering phenomenon at the outputs.

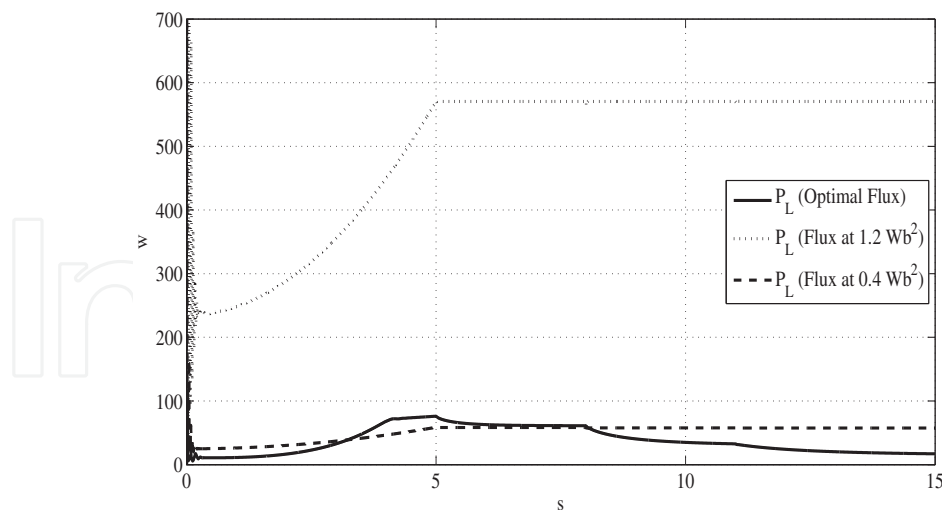
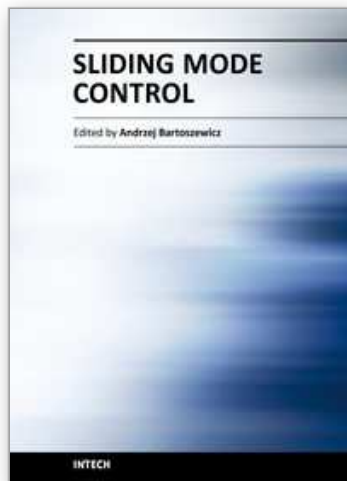


Fig. 5. Comparison of the power lost in copper and core using the optimal flux modulus, and the steady-state open-loop values for the flux modulus predicted by the classical fifth-order model and the seventh-order model here presented.

6. References

- Levant, A. (1993). Sliding order and sliding accuracy in sliding mode control, *Int. J. Control* 58(6): 1247–1263.
- Levant, A. (2005). Quasi-continuous high-order sliding-mode controllers, *IEEE Transactions on Automatic Control* 50(11): 1812–1816.
- Levant, A. & Aleshvili, L. (2007). Integral high-order sliding modes, *IEEE Transactions on Automatic Control* 52(7): 1278–1282.
- Levi, E., Boglietti, A. & Lazzar, M. (1995). Performance deterioration in indirect vector controlled induction motor drives due to iron losses, *Proc. Power Electronics Specialists Conf.*
- Moreno, J. A. & Osorio, M. A. (2008). A Lyapunov approach to second-order sliding mode controllers and observers, *Proceedings of the 47th IEEE Conference on Decision and Control*.
- Ramos, L. E., Castillo-Toledo, B. & Alvarez, J. (1997). Nonlinear regulation of an underactuated system, *International Conference on Robotics and Automation*.
- Rivera Dominguez, J., Mora-Soto, C., Ortega, S., Raygoza, J. J. & De La Mora, A. (2010). Super-twisting control of induction motors with core loss, *Variable Structure Systems (VSS), 2010 11th International Workshop on*, pp. 428–433.
- Rivera, J., Loukianov, A. & Castillo-Toledo, B. (2008). Discontinuous output regulation of the pendubot, *Proceedings of the 17th world congress The international federation of automatic control*.
- Spong, M. W. & Vidyasagar, M. (1989). *Robot Dynamics and Control*, John Wiley and Sons, Inc., New York.
- Utkin, V., Guldner, J. & Shi, . (1999). *Sliding mode control in electromechanical systems*, CRC Press.
- Utkin, V. I. (1993). Sliding mode control design principles and applications to electric drives, *IEEE Trans. Ind. Electron.* 40(1): 23–36.



Sliding Mode Control

Edited by Prof. Andrzej Bartoszewicz

ISBN 978-953-307-162-6

Hard cover, 544 pages

Publisher InTech

Published online 11, April, 2011

Published in print edition April, 2011

The main objective of this monograph is to present a broad range of well worked out, recent application studies as well as theoretical contributions in the field of sliding mode control system analysis and design. The contributions presented here include new theoretical developments as well as successful applications of variable structure controllers primarily in the field of power electronics, electric drives and motion steering systems. They enrich the current state of the art, and motivate and encourage new ideas and solutions in the sliding mode control area.

How to reference

In order to correctly reference this scholarly work, feel free to copy and paste the following:

Jorge Rivera, Luis Garcia, Christian Mora, Juan J. Raygoza and Susana Ortega (2011). Super-Twisting Sliding Mode in Motion Control Systems, Sliding Mode Control, Prof. Andrzej Bartoszewicz (Ed.), ISBN: 978-953-307-162-6, InTech, Available from: <http://www.intechopen.com/books/sliding-mode-control/super-twisting-sliding-mode-in-motion-control-systems>

INTECH
open science | open minds

InTech Europe

University Campus STeP Ri
Slavka Krautzeka 83/A
51000 Rijeka, Croatia
Phone: +385 (51) 770 447
Fax: +385 (51) 686 166
www.intechopen.com

InTech China

Unit 405, Office Block, Hotel Equatorial Shanghai
No.65, Yan An Road (West), Shanghai, 200040, China
中国上海市延安西路65号上海国际贵都大饭店办公楼405单元
Phone: +86-21-62489820
Fax: +86-21-62489821

© 2011 The Author(s). Licensee IntechOpen. This chapter is distributed under the terms of the [Creative Commons Attribution-NonCommercial-ShareAlike-3.0 License](#), which permits use, distribution and reproduction for non-commercial purposes, provided the original is properly cited and derivative works building on this content are distributed under the same license.

IntechOpen

IntechOpen